DESIGN OF H_∞ PROPORTIONAL-INTEGRAL THRUST CONTROLLER FOR RAMJET ENGINE

NEMANJA D. ZORIĆ, RADOSLAV D. RADULOVIĆ

University of Belgrade, Faculty of Mechanical Engineering, Serbia

e-mail: nzoric@mas.bg.ac.rs; rradulovic@mas.bg.ac.rs

VLADIMIR M. JAZAREVIĆ

Must Solutions, Belgrade, Serbia

e-mail: vladimir.jazarevic@mustsolutions.com

TRAJKO B. PETROVIĆ

University of Belgrade, Faculty of Electrical Engineering, Serbia

e-mail: petrovic@etf.bg.ac.rs

This paper presents the design of a thrust controller for a ramjet engine. The mathematical model for controller synthesis is based on a numerical solution of a set of nonlinear equations. Transfer functions of the engine are found for certain operation points defined by the altitude, Mach number and angle of attack. Local controllers are developed by using H_∞ control methodology, finally reduced to proportional-integral (PI) controllers. For gain scheduling, linear interpolation of parameters of the local PI controllers is used. Next, simulations are performed in order to show performances of the presented control algorithm.

Keywords: ramjet, H_∞ control, proportional-integral control, gain scheduling

1. Introduction

The ramjet presents the simplest form of air-breathing jet engines due to nonexistence of moving parts like compressors and turbines. In addition to its simplicity, it provides reasonably efficient operation over a range of supersonic speeds, altitudes and angles of attack (Chandra *et al.*, 2009, 2010). This paper presents the design of a thrust controller for a ramjet engine. The mathematical model for controller synthesis is based on a numerical solution of a set of nonlinear equations which include: conical and normal shock waves at the intake, correction for the angle of attack, pressure recovery at the diffuser, model of the combustion chamber, model of the nozzle, etc. Nonlinear simulations are performed at an altitude of 200 meters for the following Mach numbers: 2.8, 3, 3.2 and 3.4 in supercritical regimes. For each Mach number, the following angles of attack are considered: 0, 2.5 and 5.5 degrees. Thus, one operation point is determined by a single Mach number and a single angle of attack. For each operation point the simulation is run for the following fuel-to-air ratios: 0.0025, 0.005, 0.0075, 0.01, 0.015, 0.02, 0.025, 0.03, 0.035, 0.04, 0.045, 0.05 and 0.055. The following variables are simulated: thrust, fuel mass flow, air mass flow, pressure at the front of the combustion chamber and temperature in the nozzle.

Since the thrust depends on the fuel mass flow, the ramjet model can be represented in a single-input-single-output (SISO) manner. First, static relationships between the fuel mass flow and the thrust are found. Next, the first-order transfer functions for the ramjet are obtained via transient simulation for each operation point. The fuel supply system is also included in the model in the form of a 2nd order transfer function. Controllers are developed by using the H_∞ theory (Skogestad and Postlethwaite, 2001; Zhou, 1997) for each operating point resulting in 5th

order local controllers. After canceling pole-zeros pairs in the controller transfer functions, 4th order controllers are obtained. The H_∞ based controller is robust to various model uncertainties and disturbances but the resulting controller order is higher than the plant model order. Due to that, the controller may not be feasible for real-time implementation because of hardware and computational limitations (Zamani *et al.*, 2009). To avoid this problem, the obtained higher--order controllers are changed to the first-order controllers by using balance reduction. These controllers are simplified to the proportional-integral (PI) form by excluding the second term in the denominator. For gain scheduling, linear interpolation of parameters of local PI controllers is used. Next, simulations are run to present performances of the discussed control algorithm.

2.   Obtaining linear mathematical model

Dimensions of the ramjet engine elements are given in Table 1.

Table 1. Dimensions of the ramjet engine elements

Intake capture area [m^2]	0.1275
Cone angles [deg]	9; 8
Diffuser exit area [m^2]	0.12
Combustion chamber diameter [m]	0.45
Length of burning zone [m]	1.125
Nozzle throat diameter [m]	0.390
Nozzle exit diameter [m]	0.440

The thrust F of the ramjet can be calculated as follows

$$F = \dot{m}_{air}(1 + q)w_{exit} - \dot{m}_{air}M\sqrt{\kappa R T_{air}} + A_{exit}(p_{10} - p_{air}) \tag{2.1}$$

where $\dot{m}_{air}$ is the air mass flow, q is the fuel-to-air ratio, M is the Mach number, T_{air} and p_{air} are the atmospheric temperature and pressure, respectively, w_{exit} is the flow speed at the nozzle exit, A_{exit} is the cross-section area of the nozzle exit, while p_{10} is the static pressure at the nozzle exit.

The mathematical model of the ramjet engine consists of a set of nonlinear equations which include: conical and normal shock waves at the intake, correction for the angle of attack, pressure recovery at the diffuser, model of the combustion chamber, model of the nozzle, etc. This set of equations is not suitable for an analytically obtained linear model when it is necessary to calculate derivatives of the ramjet for the controller design. The mathematical model can be obtained analytically by a low-order empirical model, but this model is not capable to represent complex physical interactions in the combustion system (Chandra *et al.*, 2009, 2010). On the other hand, Computational Fluid Dynamics (CFD) provides a high-order model that is not suitable for the controller implementation. Gupta *et al.* (2007) obtained the mathematical model by a combination of CFD simulations and a quasi-1D formulation.

In this paper, the set of nonlinear equations is numerically solved by using the Newton--Raphson method (Turns, 2000). The main idea is to find the relationship between the thrust and the fuel mass flow at different operation points defined by: altitude, Mach number and angle of attack.

The non-linear model is linearized at the altitude of 200 m for each of the four Mach numbers listed in Introduction and for each of the three angles of attack also shown in Introduction. Moreover, the simulation runs for each of the thirteen fuel-to-air ratios. These operation points are listed in Introduction as well. The simulated and calculated performances are as follows: thrust,

fuel mass flow, air mass flow and temperature in the nozzle. All these simulations correspond to real supercritical regimes. Table 2 presents calculated simulation data for the operation point defined by the Mach number 3 and the angle of attack 2.5°.

From Fig. 1a it can be noticed that for a fuel mass flow below 5.92 kg/s, which corresponds to the fuel-to-air ratio of 0.04, the thrust is linear compared to the fuel mass flow. Above this value, behavior of the thrust is nonlinear. Considering Table 2, it can be concluded that for the fuel-to-air ratio above 0.04, the temperature in the nozzle is close to its critical value of 2000K. This behavior is the same for other operation points. Due to that, in further analysis, only fuel-to-air ratios below 0.04 are considered (i.e. the linear part of the curve presented in Fig. 1a). Figure 1b presents the linear part of thrust versus fuel mass flow and the trendline of the plotted values.
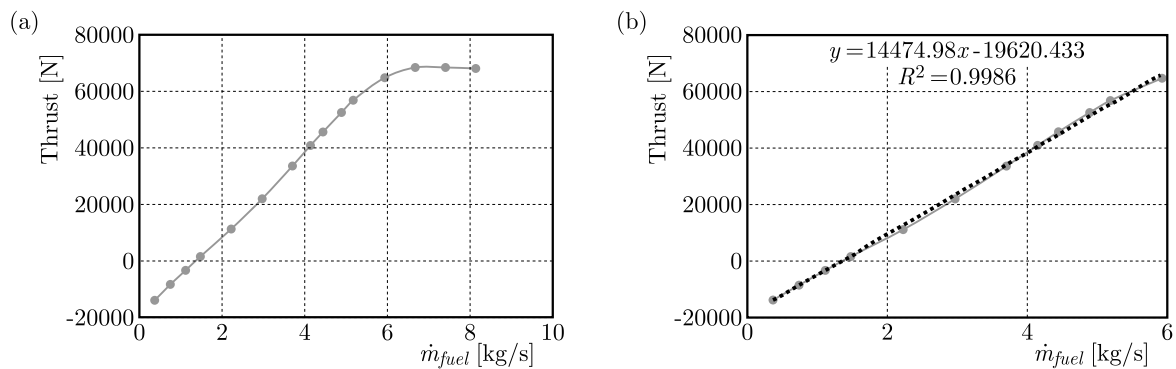

Fig. 1. $M = 3$ and $\alpha = 2.5°$: (a) thrust versus fuel mass flow, (b) linear part of thrust versus fuel mass flow and trendline

Table 2. Calculated data from nonlinear simulation for $M = 3$ and $\alpha = 2.5°$

q	F [N]	$\dot{m}_{fuel}$ [kg/s]	$\dot{m}_{air}$ [kg/s]	T_{10} [K]
0.0025	-13736.8	0.37	148.005	903.3095
0.005	-8358.09	0.74	148.005	963.5276
0.0075	-3269.78	1.11	148.005	1021.721
0.01	1579.941	1.48	148.005	1078.244
0.015	11199.32	2.22	148.005	1193.884
0.02	21705.93	2.96	148.005	1326.718
0.025	33443.39	3.70	148.005	1483.43
0.028	40772.36	4.144	148.005	1585.272
0.03	45584.52	4.44	148.005	1653.548
0.033	52405.16	4.884	148.005	1751.754
0.035	56513.49	5.18	148.005	1811.315
0.04	64455.67	5.92	148.005	1924.402
0.045	68205.96	6.66	148.005	1968.621
0.05	68164	7.40	148.005	1949.216
0.055	68012.18	8.14	148.005	1928.281

Using the obtained data, the thrust is plotted against the fuel mass flow. Fig. 1a presents the thrust versus fuel mass flow for the operation point defined by the Mach number 3 and the angle of attack 2.5°.

Thus, the static relation between the thrust and the fuel mass flow can be represented as follows

$$F = G_{rj}\dot{m}_{fuel} + C_0 \tag{2.2}$$

where G_{rj} and C_0 are constants which can be determined from the trendlines. The previously obtained dependence between the thrust and the fuel mass flow corresponds to the static behavior of the ramjet engine. The part of the engine that contributes to engine dynamics is the combustion chamber. Dynamical behavior of the combustion chamber can be modeled by using the following first-order differential equation

$$\dot{p}_7 = \frac{\dot{m}_7 - \dot{m}_8}{B} \tag{2.3}$$

where p_7 and $\dot{m}_7$ are the pressure and the mass flow at the front of the combustion chamber, $\dot{m}_8$ is the mass flow at the exit of the combustion chamber, while B is the backpressure factor given as

$$B = \Big(\int\limits_7^8 \frac{1}{\gamma R T(x)}\, dx\Big) A_{com} \tag{2.4}$$

where γ is the heat capacity ratio, R is the specific gas constant, $T(x)$ is the static temperature at location x, while A_{com} is the cross-section area of the combustion chamber.

Equation (2.3) is solved numerically by using transient simulation. The transient simulation calculates variation of the pressure in front of the combustion chamber versus time for a given step input of fuel mass flow and is performed for each operating point for the following intervals of fuel-to-air ratios: 0.00001-0.005; 0.005-0.01; 0.01-0.015; 0.015-0.02; 0.02-0.025; 0.025-0.03; 0.03-0.035; 0.035-0.04. Afterwards, the pressure in front of the combustion chamber is adjusted to start with the zero value at the initial time by removing the off-set (i.e. subtracting the first value from all values). In other words, an increment of this pressure is obtained. Figure 2a presents the step response of this pressure for the operating point defined by the Mach number 3 and the angle of attack 2.5° with an input step-function of the fuel-to-air ratio from 0.025 to 0.03.
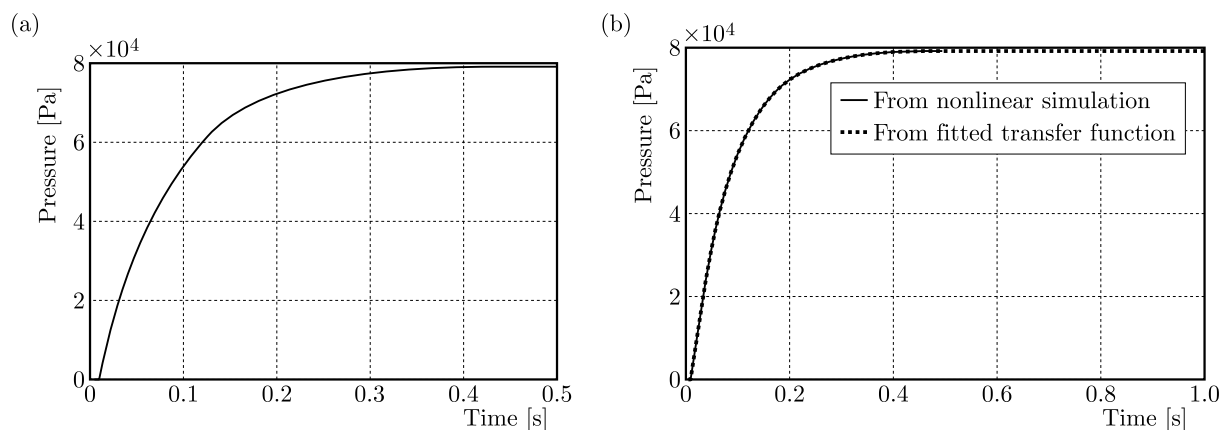

Fig. 2. Step response for $M = 3$, $\alpha = 2.5°$ and $q = 0.025$-0.03: (a) from nonlinear simulation, (b) comparison from nonlinear simulation and obtained from fitted transfer function

This response can be modeled as the first-order transfer function. The input in this transfer function is a step function of increment of the pressure (from 0 to Δp_{7max}). Thus, the transfer function can be represented as follows

$$H(s) = \frac{1}{\tau s + 1} \tag{2.5}$$

where τ is the time constant which depends on the operation point as well as on the fuel-to-air ratio. It will be determined iteratively in such way so as to minimize the deviation between the graph obtained as the output of the transfer function and the graph obtained by the transient response from the nonlinear model. For example, considering the step response presented by Fig. 2a, the fitted value of τ is 0.078, and these two graphs are presented by Fig. 2b.

Since the thrust depends on the pressure in front of the combustion chamber and its transient behavior corresponds to transient behavior of this pressure, the relation between the thrust and the fuel mass flow can be represented as follows

$$F = \frac{G_{rj}}{\tau s + 1}\dot{m}_{fuel} + C_0 \tag{2.6}$$

The input/output form of the previous equation can be written as

$$\delta F = \frac{G_{rj}}{\tau s + 1}\delta \dot{m}_{fuel} \tag{2.7}$$

so, the transfer function of the ramjet engine is

$$H_{rj}(s) = \frac{G_{rj}}{\tau s + 1} \tag{2.8}$$

The obtained values of the parameters of equation (2.5) are shown in Tables 3 and 4.

Table 3. Obtained values of G_{rj} and C_0

M	$\alpha\ [^\circ]$	G_{rj}	C_0
	0	14845.58	-14880.23
2.8	2.5	14845.11	-14892.44
	5.5	14859.97	-15002.95
	0	14475.43	-19634.06
3	2.5	14474.981	-19620.433
	5.5	14453.53	-19493.39
	0	14102.94	-25426.3
3.2	2.5	14102.5	-25381.29
	5.5	14099.79	-25108.14
	0	13730.86	-32330.66
3.4	2.5	13730.45	-32248.34
	5.5	13727.86	-31748.8

The fuel pump model can be represented as the second-order transfer function (Chandra *et al.*, 2009, 2010)

$$H_{fss}(s) = \frac{\dot{m}_{fuel}(s)}{i(s)} = \frac{K_c \omega_n^2}{s^2 + 2\zeta\omega_n s + \omega_n^2} \tag{2.9}$$

where $K_c = 2.4$, $\omega_n = 1507.96$ and $\zeta = 0.5$ are the low-frequency (DC) gain, the natural frequency and the damping ratio of the fuel pump transfer function, respectively, and i represents current as the control input in the metering valve.

3. Control system design

3.1. H_∞ control design

A block diagram of the designed closed loop is shown in Fig. 3.

Table 4. Obtained values of τ

| M	α [°]	q							
		0.00001- -0.005	0.005- -0.01	0.01- -0.015	0.015- -0.02	0.02- -0.025	0.025- -0.03	0.03- -0.035	0.035- -0.04
2.8	0	0.07	0.066	0.066	0.075	0.088	0.088	0.078	0.05
	2.5	0.072	0.066	0.067	0.075	0.088	0.088	0.078	0.05
	5.5	0.072	0.067	0.068	0.075	0.088	0.088	0.078	0.05
3	0	0.062	0.058	0.058	0.066	0.076	0.078	0.068	0.044
	2.5	0.062	0.058	0.058	0.066	0.077	0.078	0.068	0.045
	5.5	0.062	0.058	0.059	0.068	0.077	0.078	0.068	0.046
3.2	0	0.054	0.05	0.05	0.058	0.066	0.068	0.06	0.04
	2.5	0.054	0.05	0.052	0.058	0.067	0.068	0.06	0.04
	5.5	0.054	0.051	0.052	0.058	0.067	0.068	0.06	0.042
3.4	0	0.047	0.044	0.044	0.052	0.06	0.06	0.052	0.032
	2.5	0.047	0.044	0.045	0.052	0.06	0.061	0.053	0.034
	5.5	0.047	0.044	0.045	0.052	0.06	0.062	0.053	0.036
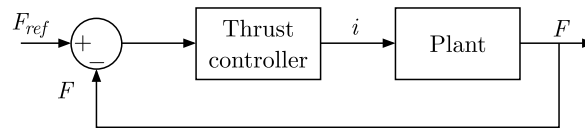
Fig. 3. Block diagram of the designed closed loop; F_{ref} is the reference thrust

The plant model consists of the ramjet engine and the fuel supply system, so the control input in the plant is the current, while the output is the thrust. The transfer function of the plant can be calculated as follows

$$H_{pl}(s) = H_{rj}(s)H_{fss}(s) \tag{3.1}$$

The H_∞ controller is designed by using the S/KS mixed-sensitivity approach (Skogestad and Postlethwaite, 2001). This approach enables obtaining H_∞ by simultaneously shaping frequency responses for reference tracking, disturbance rejection, robustness, and control effort. The input--output relation of the S/KS mixed sensitivity minimization model (Skogestad and Postlethwaite, 2001) is displayed in Fig. 4.
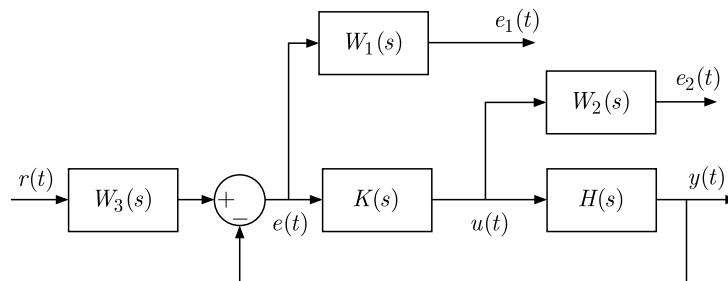

Fig. 4. Input-output relation of the S/KS mixed sensitivity minimization model

In Fig. 4, $r(t)$ is the reference input, $e(t)$ – error signal, $y(t)$ – output variable, $u(t)$ – control input (controller output), $K(s)$ – H_∞ controller, $W_1(s)$, $W_2(s)$ and $W_3(s)$ are weighting functions which reflect the system performance requirements (reference tracking and control effort), $H_{pl}(s)$ is the plant transfer function, while $e_1(t)$ and $e_2(t)$ are weighted outputs.

The selection of weighting functions for a specific design problem involves many iterations, fine tuning and trial-and-error procedure, and it is very hard to give a general equation that will work for every problem (Zhou, 1997). In the design procedure presented in this paper, the following weighting functions are selected by using the trial-and-error procedure

$$W_1(s) = 0.5\frac{s + 12}{s + 0.012} \qquad W_2(s) = 0.5\frac{s + 0.0001}{s + 10} \qquad W_3(s) = 1 \qquad (3.2)$$

Since the plant model depends on the operating point as well as on the fuel-to-air ratio, the main idea is to design a controller for each operating point (local controllers) and perform gain scheduling of the controller parameters. By scheduling these parameters, the robustness and performance for the whole envelope can be evaluated. In order to reduce the number of local controllers and also considering the robustness of H_∞ control, instead of calculating the controller for each interval of the fuel-to-air ratio for a certain operation point, the average of the parameter τ is used. Since the thrust is negative for the intervals of the fuel-to-air ratio 0.00001-0.005 and 0.005-0.01, these intervals are excluded for determination of the average of τ. Thus the obtained transfer functions of the ramjet for H_∞ synthesis are presented in Table 5.

Table 5. Transfer functions of the ramjet of each operating point for H_∞ synthesis

M	$\alpha = 0°$	$\alpha = 2.5°$	$\alpha = 5.5°$
2.8	$\frac{14845.58}{0.0742s+1}$	$\frac{14845.11}{0.0743s+1}$	$\frac{14859.97}{0.0794s+1}$
3	$\frac{14475.43}{0.065s+1}$	$\frac{14474.98}{0.0653s+1}$	$\frac{14453.53}{0.066s+1}$
3.2	$\frac{14102.94}{0.057s+1}$	$\frac{14102.50}{0.0575s+1}$	$\frac{14099.79}{0.0578s+1}$
3.4	$\frac{13730.86}{0.05s+1}$	$\frac{13730.45}{0.0508s+1}$	$\frac{13727.86}{0.0518s+1}$

Considering orders of the ramjet and the fuel supply system, the plant model is the 3-rd order model. Also, weights W_1 and W_2 are the 1st order transfer functions, which results in the 5th order controllers. After canceling pole-zeros pairs in the controller transfer function, the 4th order controllers can be obtained. After eliminating negligible states by using the balanced reduction, obtained controllers can be reduced to the lower orders. In this case, the controllers are reduced to the 1st order. The transfer functions of the local non-reduced and reduced controllers are presented in Table 6.

For the operating point defined by the Mach number 3 and the angle of attack 2.5°, Fig. 5a presents singular values, Fig. 5b presents the step response from the reference to the output, while Fig. 5c presents the step response from the reference to the input for the non-reduced and reduced controller.

3.2. Obtaining PI controllers and gain scheduling

From Table 5 it can be noticed that for reduced controllers the second term in the denominator (0.012) is much smaller than the first term (1), so it can be omitted. In that case, PI controllers can be obtained. Table 7 presents proportional gains K_p and integral gains K_i of the obtained local PI controllers for each operation point.

For gain scheduling, linear interpolation of the parameters of local PI controllers is used. Also, for simulation, linear interpolation of the ramjet model parameters (Tables 3 and 4) is used.

Table 6. Transfer functions of local controllers

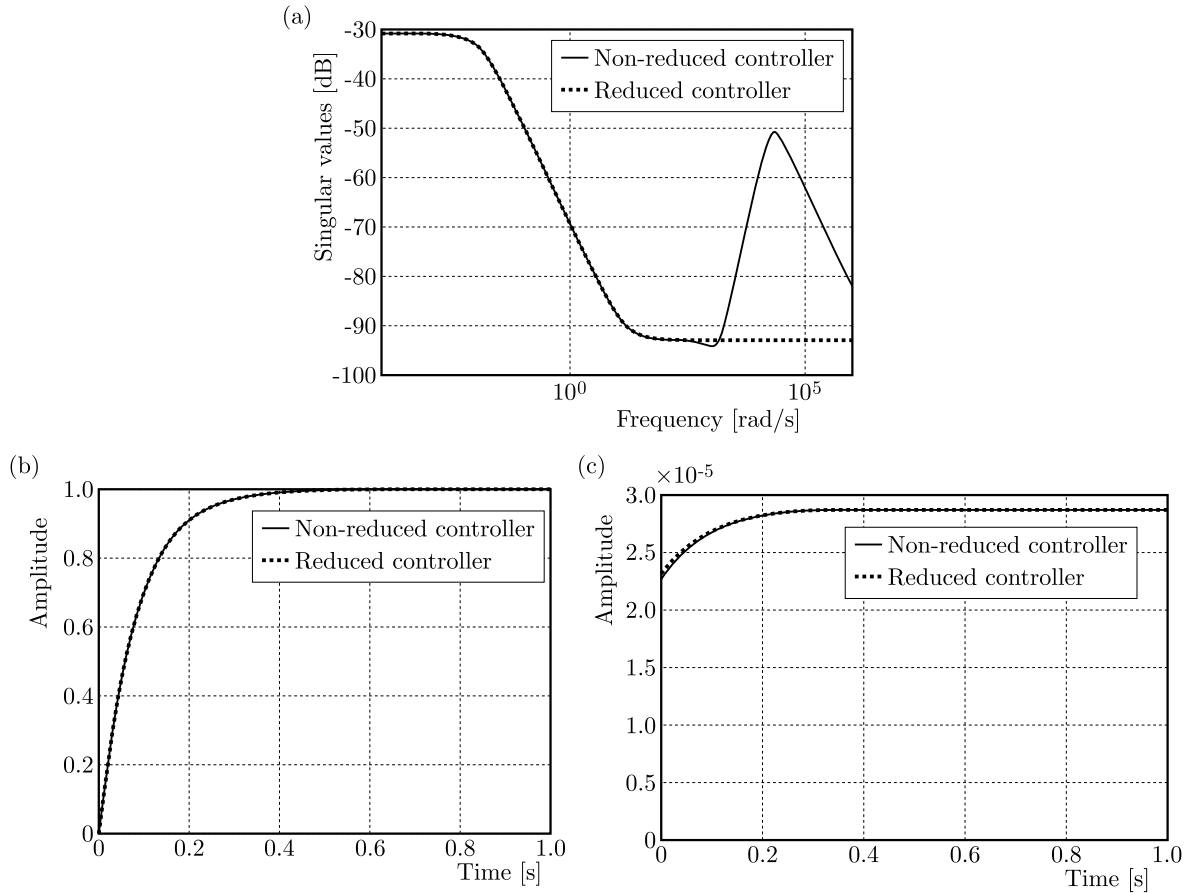| M	α [°]	Non-reduced controllers	Reduced controllers
2.8	0	$\dfrac{78.52s^3+1.195\cdot10^5s^2+1.802\cdot10^8s+2.408\cdot10^9}{s^4+3.836\cdot10^4s^3+7.369\cdot10^8s^2+7.164\cdot10^{12}s+8.597\cdot10^{10}}$	$\dfrac{2.511\cdot10^{-5}s+0.000336}{s+0.012}$
	2.5	$\dfrac{78.52s^3+1.195\cdot10^5s^2+1.802\cdot10^8s+2.402\cdot10^9}{s^4+3.833\cdot10^4s^3+7.358\cdot10^8s^2+7.148\cdot10^{12}s+8.578\cdot10^{10}}$	$\dfrac{2.517\cdot10^{-5}s+0.0003361}{s+0.012}$
	5.5	$\dfrac{78.57s^3+1.195\cdot10^5s^2+1.802\cdot10^8s+2.25\cdot10^9}{s^4+3.752\cdot10^4s^3+7.048\cdot10^8s^2+6.703\cdot10^{12}s+8.043\cdot10^{10}}$	$\dfrac{2.684\cdot10^{-5}s+0.0003357}{s+0.012}$
3	0	$\dfrac{78.45s^3+1.195\cdot10^5s^2+1.802\cdot10^8s+2.745\cdot10^9}{s^4+3.975\cdot10^4s^3+7.91\cdot10^8s^2+7.963\cdot10^{12}s+9.556\cdot10^{10}}$	$\dfrac{2.26\cdot10^{-5}s+0.0003447}{s+0.012}$
	2.5	$\dfrac{78.46s^3+1.195\cdot10^5s^2+1.802\cdot10^8s+2.731\cdot10^9}{s^4+3.968\cdot10^4s^3+7.883\cdot10^8s^2+7.923\cdot10^{12}s+9.507\cdot10^{10}}$	$\dfrac{2.271\cdot10^{-5}s+0.0003447}{s+0.012}$
	5.5	$\dfrac{78.46s^3+1.195\cdot10^5s^2+1.802\cdot10^8s+2.703\cdot10^9}{s^4+3.953\cdot10^4s^3+7.822\cdot10^8s^2+7.832\cdot10^{12}s+9.398\cdot10^{10}}$	$\dfrac{2.298\cdot10^{-5}s+0.0003452}{s+0.012}$
3.2	0	$\dfrac{78.39s^3+1.196\cdot10^5s^2+1.803\cdot10^5s+3.127\cdot10^9}{s^4+4.116\cdot10^4s^3+8.482\cdot10^8s^2+8.839\cdot10^{12}s+1.061\cdot10^{11}}$	$\dfrac{2.037\cdot10^{-5}s+0.0003538}{s+0.012}$
	2.5	$\dfrac{78.39s^3+1.196\cdot10^5s^2+1.803\cdot10^8s+3.1\cdot10^9}{s^4+4.104\cdot10^4s^3+8.433\cdot10^8s^2+8.763\cdot10^{12}s+1.052\cdot10^{11}}$	$\dfrac{2.054\cdot10^{-5}s+0.0003538}{s+0.012}$
	5.5	$\dfrac{78.4s^3+1.196\cdot10^5s^2+1.803\cdot10^8s+3.082\cdot10^9}{s^4+4.096\cdot10^4s^3+8.399\cdot10^8s^2+8.711\cdot10^{12}s+1.045\cdot10^{11}}$	$\dfrac{2.066\cdot10^{-5}s+0.0003539}{s+0.012}$
3.4	0	$\dfrac{78.32s^3+1.197\cdot10^5s^2+1.805\cdot10^8s+3.562\cdot10^9}{s^4+4.261\cdot10^4s^3+9.09\cdot10^8s^2+9.803\cdot10^{12}s+1.176\cdot10^{11}}$	$\dfrac{1.838\cdot10^{-5}s+0.0003634}{s+0.012}$
	2.5	$\dfrac{78.33s^3+1.197\cdot10^5s^2+1.804\cdot10^8s+3.504\cdot10^9}{s^4+4.238\cdot10^4s^3+8.991\cdot10^8s^2+9.643\cdot10^{12}s+1.157\cdot10^{11}}$	$\dfrac{1.868\cdot10^{-5}s+0.0003634}{s+0.012}$
	5.5	$\dfrac{78.34s^3+1.197\cdot10^5s^2+1.804\cdot10^8s+3.47\cdot10^9}{s^4+4.224\cdot10^4s^3+8.931\cdot10^8s^2+9.548\cdot10^{12}s+1.146\cdot10^{11}}$	$\dfrac{1.886\cdot10^{-5}s+0.0003635}{s+0.012}$

Fig. 5. Comparisons of non-reduced and reduced controller for the operating point $M = 3$ and $\alpha = 2.5°$: (a) singular values of controllers, (b) step response from the reference to output, (c) step response from the reference to input

Table 7. Proportional and integral gains of local PI controllers

M	α [°]	K_p	K_i
2.8	0	$2.511 \cdot 10^{-5}$	0.000336
	2.5	$2.517 \cdot 10^{-5}$	0.0003361
	5.5	$2.684 \cdot 10^{-5}$	0.0003357
3	0	$2.26 \cdot 10^{-5}$	0.0003447
	2.5	$2.271 \cdot 10^{-5}$	0.0003447
	5.5	$2.298 \cdot 10^{-5}$	0.0003452
3.2	0	$2.037 \cdot 10^{-5}$	0.0003538
	2.5	$2.054 \cdot 10^{-5}$	0.0003538
	5.5	$2.066 \cdot 10^{-5}$	0.0003539
3.4	0	$1.838 \cdot 10^{-5}$	0.0003634
	2.5	$1.868 \cdot 10^{-5}$	0.0003634
	5.5	$1.886 \cdot 10^{-5}$	0.0003635

4. Simulation results

Simulations are performed for two operation regimes. The first regime is defined as:

- 0 s-10 s: Mach number is 2.9, angle of attack is 5° and reference thrust is 30000 N;
- 10 s-20 s: Mach number is linearly varied from 2.9 to 3.3, angle of attack is linearly varied from 5° to 1° and reference thrust is 60000 N;
- 20 s: Mach number is 3.3, angle of attack is 1° and reference thrust is 50000 N.

The variation of the Mach number and angle of attack versus time is presented in Fig. 6. Figure 7a shows the obtained thrust compared to the reference thrust versus time, while Fig. 7b shows the fuel mass flow and the-fuel-to-air ratio versus time.
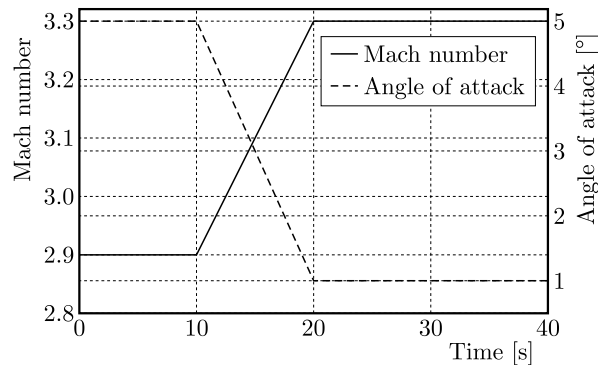

Fig. 6. Variation of the Mach number and angle of attack versus time

In the second regime, the Mach number, the angle of attack and the reference thrust are varied as a sine function, as follows (α [°], F_{ref} [N])

$$M = 3.1 + 0.3\sin(0.1t) \qquad \alpha = 2.75 + 2.75\sin(0.075t)$$
$$F_{ref} = 30000 + 20000\sin(0.15t)$$

(4.1)

The obtained thrust compared to the reference thrust versus time is presented in Fig. 8a. Figure 8b shows fuel mass flow and the fuel-to-air ratio versus time.

According to Fig. 7 and Fig. 8, it can be concluded that all specifications are satisfied and the presented control algorithm shows good performances regarding the reference tracking.
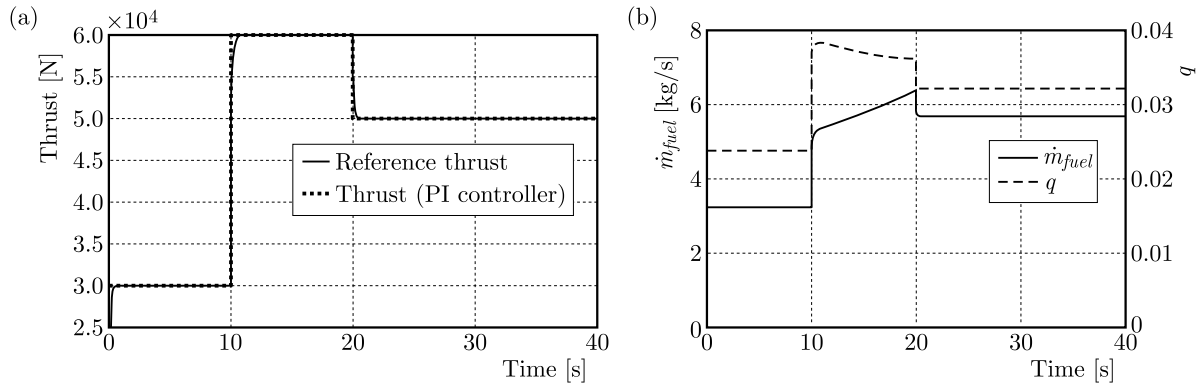
Fig. 7. PI controller, simulation results for the first regime: (a) obtained thrust compared to the reference thrust versus time, (b) fuel mass flow and the fuel-to-air ratio versus time
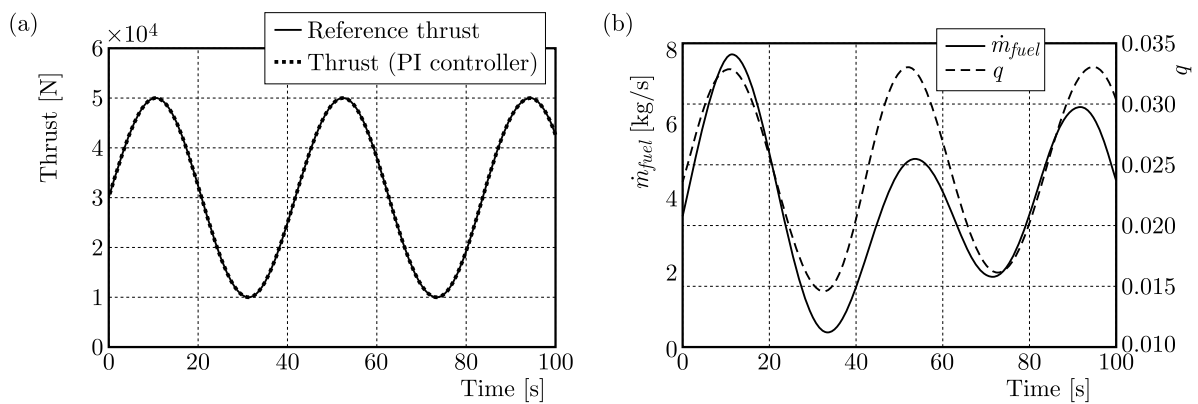

Fig. 8. PI controller, simulation results for the second regime: (a) obtained thrust compared to the reference thrust versus time, (b) fuel mass flow and the fuel-to-air ratio versus time

5. Conclusion

The paper presents the design of a thrust controller for the ramjet engine. From the mathematical model, the transfer function of the engine is found for certain operation points defined by the altitude, Mach number and angle of attack. The fuel supply system is also included in the model. Controllers for each operation point (local controllers) are developed by using the H_∞ methodology. The obtained 4th order controllers are reduced to the 1st order controllers by using balance reduction and, thereafter, the controllers are reduced to PI controllers. For gain scheduling, linear interpolation of the parameters of local the PI controllers is used. Simulations are performed for linear and sinusoidal variation of the Mach number, angle of attack and reference thrust. The obtained simulation results show that the obtained control algorithm provides good performances regarding the reference tracking.

References

1. CHANDRA K.P.B, GUPTA N.K., ANANTHKRISHNAN N., PARK I.S., YOON H.G., 2010, Modeling, simulation, and controller design for an air-breathing combustion system, *Journal of Propulsion and Power*, **26**, 3, 562-574

2. CHANDRA K.P.B, GUPTA N.K., ANANTHKRISHNAN N., RENGANATHAN V.S., PARK I.S., YOON H.G., 2009, Modeling, dynamic simulation and controller design for an air-breathing combustion system, *47th AIAA Aerospace Science Meeting and The New Horizons Forum and Aerospace Exhibit*, Orlando, Florida

3. GUPTA N.K., GUPTA B.K., ANANTHKRISHNAN N., SHEVARE G.R., PARK I.S., YOON H.G., 2007, Integrated modeling and simulation of an air-breathing combustion system dynamics, AIAA Paper 2007-6374, *AIAA Modeling and Simulation Technologies Conference and Exhibit*, Hilton Head, South Carolina

4. SKOGESTAD S., POSTLETHWAITE I., 2001, *Multivariable Feedback Control: Analysis and Design*, 2nd Edition, John Wiley & Sons

5. TURNS S.R., 2000, *An Introduction to Combustion: Concepts and Applications*, 2nd Edition, McGraw-Hill Education

6. ZAMANI M., SADATI N., GHARTEMANI M.K., 2009, Design of an H_∞ PID controller using particle swarm optimization, *International Journal of Control, Automation, and Systems*, **7**, 2, 273-80

7. ZHOU K., 1997, *Essentials of Robust Control*, 1st Edition, Pearson